



Use of ^{99m}Tc -sestamibi SPECT/CT imaging in predicting the degree of pathological hyperplasia of the parathyroid gland: semi-quantitative analysis

Junhao Ma¹, Jun Yang², Chuanzhi Chen¹, Yimin Lu¹, Zhuochao Mao¹, Haohao Wang¹, Yan Yang¹, Zhongqi Li¹, Weibin Wang¹, Lisong Teng¹

¹Department of Surgical Oncology, First Affiliated Hospital, Zhejiang University, Hangzhou, China; ²Department of Nuclear Medicine, First Affiliated Hospital, Zhejiang University, Hangzhou, China

Contributions: (I) Conception and design: J Ma, W Wang, L Teng; (II) Administrative support: L Teng; (III) Provision of study materials or patients: J Yang, Y Lu, Z Mao, Z Li, H Wang; (IV) Collection and assembly of data: J Ma, Y Yang, J Yang, C Chen; (V) Data analysis and interpretation: J Ma, J Yang, W Wang, C Chen; (VI) Manuscript writing: All authors; (VII) Final approval of manuscript: All authors.

Correspondence to: Lisong Teng, PhD; Weibin Wang, PhD. #79 Qingchun Road, Shangcheng District, Hangzhou, China. Email: lsteng@zju.edu.cn; wbwang@zju.edu.cn.

Background: Previous studies have demonstrated that ^{99m}Tc -sestamibi (^{99m}Tc -MIBI) Single-Photon Emission Computed Tomography/ Computed Tomography (SPECT/CT) imaging is an effective isotopic technique for locating the parathyroid in secondary hyperparathyroidism (SHPT). This study aimed to explore further the correlation between ^{99m}Tc -MIBI SPECT/CT imaging and SHPT to demonstrate the value of ^{99m}Tc -MIBI SPECT/CT in evaluating the degree of pathological hyperplasia of the parathyroid gland (PG).

Methods: The demographics, surgical records, and follow-up information of 91 patients were recorded and analyzed. A total of 216 paraffin-embedded PGs of 54 patients were obtained and analyzed.

Results: Patients with ^{99m}Tc -MIBI negative PG(s) had significantly lower preoperative serum phosphorus and higher serum calcium levels at 6 months postoperatively compared to those with ^{99m}Tc -MIBI positive PG(s) ($P<0.05$). We also found a higher total uptake ratio of the region of interest (URRI) and higher URRI max in the hypocalcemia group than in the non-hypocalcemia group. Both URRI total ($P=0.003$) and URRI max ($P=0.028$) were independent risk factors for hypocalcemia 6 months postoperatively. The URRI values of the PGs were significantly positively correlated with glandular weight ($R^2=0.343$, $P<0.001$), glandular volume ($R^2=0.240$, $P<0.001$), and degree of pathological hyperplasia ($P<0.001$). However, the URRI value of the PGs exhibited a notably weak correlation with proliferating cell nuclear antigen (PCNA) ($R^2=0.035$, $P=0.006$). The area under the receiver operating characteristic curve showed a URRI evaluative value of 0.771 for diffuse and nodular types in 216 PGs ($P<0.001$). We further evaluated 167 nodular-type PGs, distinguishing between nodular hyperplasia and a single nodule; the URRI evaluative value reached 0.819, which was higher than the volume or weight ($P<0.001$).

Conclusions: The ^{99m}Tc -MIBI SPECT/CT scintigraphy results were related to serum calcium levels at 6 months after total parathyroidectomy with autotransplantation (TPTX+AT), suggesting the occurrence of hypocalcemia (6 months after TPTX+AT). More importantly, this technique effectively evaluated the pathological hyperplasia of PGs preoperatively, and therefore, could assist surgeons in selecting the PGs with the lowest degree of hyperplasia intraoperatively.

Keywords: ^{99m}Tc -MIBI; hyperplasia; parathyroid gland; secondary hyperparathyroidism; hypocalcemia

Submitted Jan 17, 2021. Accepted for publication May 19, 2021.

doi: 10.21037/qims-21-66

View this article at: <http://dx.doi.org/10.21037/qims-21-66>

Introduction

Uremic secondary hyperparathyroidism is a complicated disease with multifactorial conditions and protean clinical manifestations that occur in most patients with advanced chronic kidney disease. Phosphate accumulation and the trend of hypocalcemia are continuous stimulations that contribute to the development and progression of hyperparathyroidism, leading to abnormal mineral metabolisms, such as metabolic bone disease and extraosseous calcification. These factors result in a poor quality of life and short life expectancy in patients with secondary hyperparathyroidism (SHPT) (1,2). In the early stages, the development of SHPT can be controlled by maintenance dialysis or pharmacotherapy (3,4). However, with the progress of the disease, surgical intervention is required when drug therapy becomes ineffective or parathyroid hormone (PTH) levels exceed a certain range (5,6). The surgical methods of parathyroidectomy include total parathyroidectomy (TPTX), subtotal parathyroidectomy (SPTX), and total parathyroidectomy with autotransplantation (TPTX+AT). Each surgical approach has its advantages and limitations, and it should be selected based on the management of dialysis and the patient's characteristics (7,8).

When performing an SPTX, the partial parathyroid gland (PG) with the lowest degree of hyperplasia among all PGs needs to be selected for preservation *in situ* while the others are resected. TPTX+AT refers to selecting the partial PG with the lowest degree of hyperplasia based on total parathyroidectomy and cutting it into 1 mm³ (approximately) for autotransplantation. Due to the heterogeneity of the PGs, the intraoperative frozen section diagnosis of a PG just is a reference for the remaining PG that is preserved *in situ* or autotransplantation. Preoperatively, a few non-invasive examinations can help to select the PG with the lowest degree of hyperplasia (9). According to previous studies, the percentage of recurrence caused by implanted PG tissue is approximately 13–60% (10,11).

^{99m}Tc -sestamibi (^{99m}Tc -MIBI) Single-Photon Emission Computed Tomography/Computed Tomography (SPECT/CT) imaging is an effective preoperative examination in

SHPT, which can provide accurate locations of hyperplasia PGs and their relationship with adjacent tissues (12). Moreover, it is more precise for locating hyperplastic PGs than ultrasonography, with a sensitivity of 70.30%, which is higher than that of ultrasonography (61.82%) (13). Therefore, we found that the degree of ^{99m}Tc -MIBI accumulation is related to the degree of pathological hyperplasia of the PGs in patients before surgery, which helps us to preserve the PG with the lowest degree of hyperplasia in SPTX or TPTX+AT intraoperatively.

This study retrospectively analyzed the relationship between ^{99m}Tc -MIBI SPECT/CT imaging and hyperplastic PGs' clinical and pathological characteristics. We aimed to explore the clinical significance and value of ^{99m}Tc -MIBI SPECT/CT scintigraphy in SHPT by evaluating the identification of the pathological hyperplasia of PGs.

Methods

Patients and methods

A total of 96 SHPT patients who underwent TPTX+AT at the First Affiliated Hospital of Zhejiang University from May 2019 to January 2020 were retrospectively enrolled. Patients with primary hyperparathyroidism, tertiary hyperparathyroidism, and multiple endocrine neoplasms were excluded. All matched 96 patients were initially treated at our institution without any previous head and neck surgery or radiation history. All patients had received a successful operation, which was defined as a serum intact parathyroid hormone (iPTH) level <300 pg/mL in the first postoperative week, following previous studies (14). iPTH concentrations were measured using chemiluminescence. Serum calcium and serum phosphorus level were measured using the colorimetric method.

Ninety-six patients were followed up, and five were lost to follow-up. Thus, the demographics, surgical records, and follow-up information of 91 patients were recorded and analyzed. Also, a total of 216 paraffin-embedded PGs of 54 patients were obtained and analyzed. Among these 54 patients, three parathyroids were removed in two patients, four were removed in 50 patients, and five were removed in two patients. Meanwhile, the preoperative ^{99m}Tc -MIBI

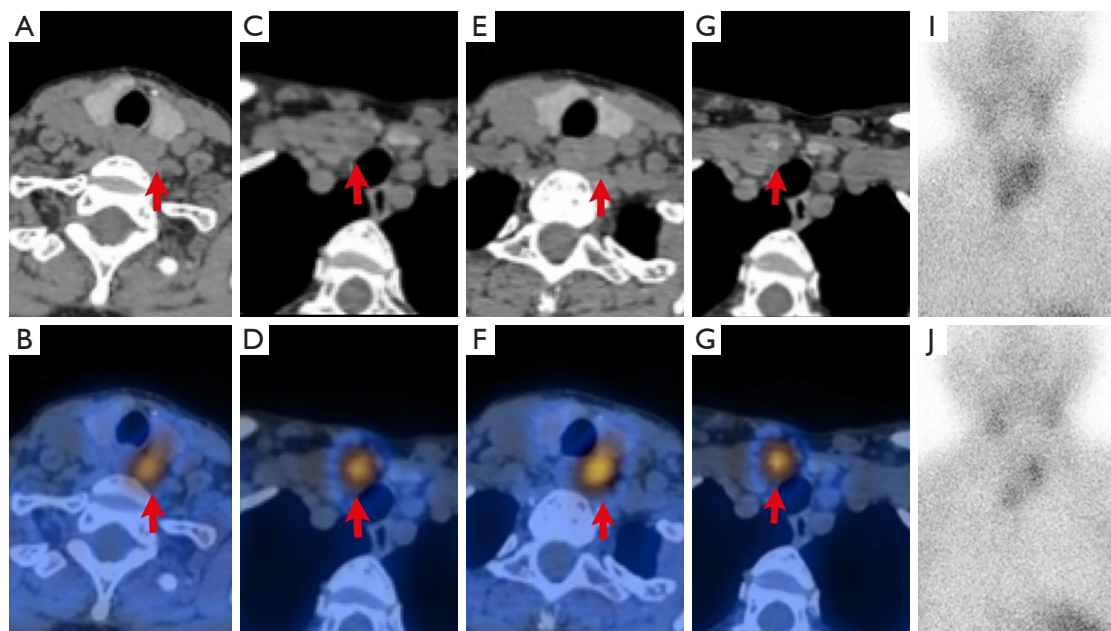


Figure 1 Axial CT (A,C,E,G) and SPECT/CT (B,D,F,H) showed four lesions in the back of the thyroid gland that were pathologically confirmed to be parathyroid hyperplasia (A,B: superior left parathyroid gland; C,D: inferior left parathyroid gland; E,F: superior right parathyroid gland; G,H: inferior right parathyroid gland). The early and delayed phase planar images (I,J) showed ^{99m}Tc -MIBI uptake of the thyroid lobe and parathyroid gland.

SPECT/CT imaging results of these patients were also available.

This study was conducted following the Declaration of Helsinki (as revised in 2013) and was approved by the institutional of Clinical Research Ethics Committee of the First Affiliated Hospital, Zhejiang University School of Medicine (No. IIT20200715). The requirement for individual consent for this retrospective analysis was waived.

Surgical approach

All patients underwent TPTX+AT surgery. During the operation, all PGs of the patients were explored and resected, and the partial PGs with the lowest degree of hyperplasia were selected and cut into 1 mm^3 . Two sites were selected for autotransplantation in the forearm muscles of the non-fistula hand (5,15,16).

^{99m}Tc -MIBI scintigraphy

^{99m}Tc -MIBI scintigraphy was performed using a SPECT/CT scanner (GE Medical Systems, 670, Tirat Hacarmel, Israel) after intravenous administration of 740 MBq

^{99m}Tc -MIBI (Figures 1,2). Planar images of the neck and mediastinum were performed for 15 min (early image) and 120 min (delayed image). The planar images were obtained in a 128×128 matrix with a 20% window centered on the 140-keV photopeak with a low-energy, high-resolution parallel collimator. After delayed image acquisition, SPECT/CT was immediately performed with 64 frames over 360° ; 20 s/frame; 20% window centered around a 140 keV photopeak; window matrix, 128×128 ; and zoom, 1. The CT acquisition parameters were as follows: 120 kV; 100–440 mA by automatic exposure control; pitch, 0.938; helical thickness, 1.25 mm; detector configuration, 2.5 mm; and beam-width, 2.5 mm. ^{99m}Tc -MIBI scintigraphy and SPECT/CT were analyzed at a workstation (Xeleris™, GE Healthcare) that was displayed in the transaxial, coronal, and sagittal slices of the CT, SPECT, and fused SPECT/CT images. Two experienced nuclear medicine doctors evaluated the images and reached a final consensus.

The precise location of each focus was reported according to the midline of the thyroid, and abnormal parathyroid lesions were divided into four quadrants. The regions of interest in the PG and the ipsilateral thymus lesion were manually delineated on the SPECT/CT

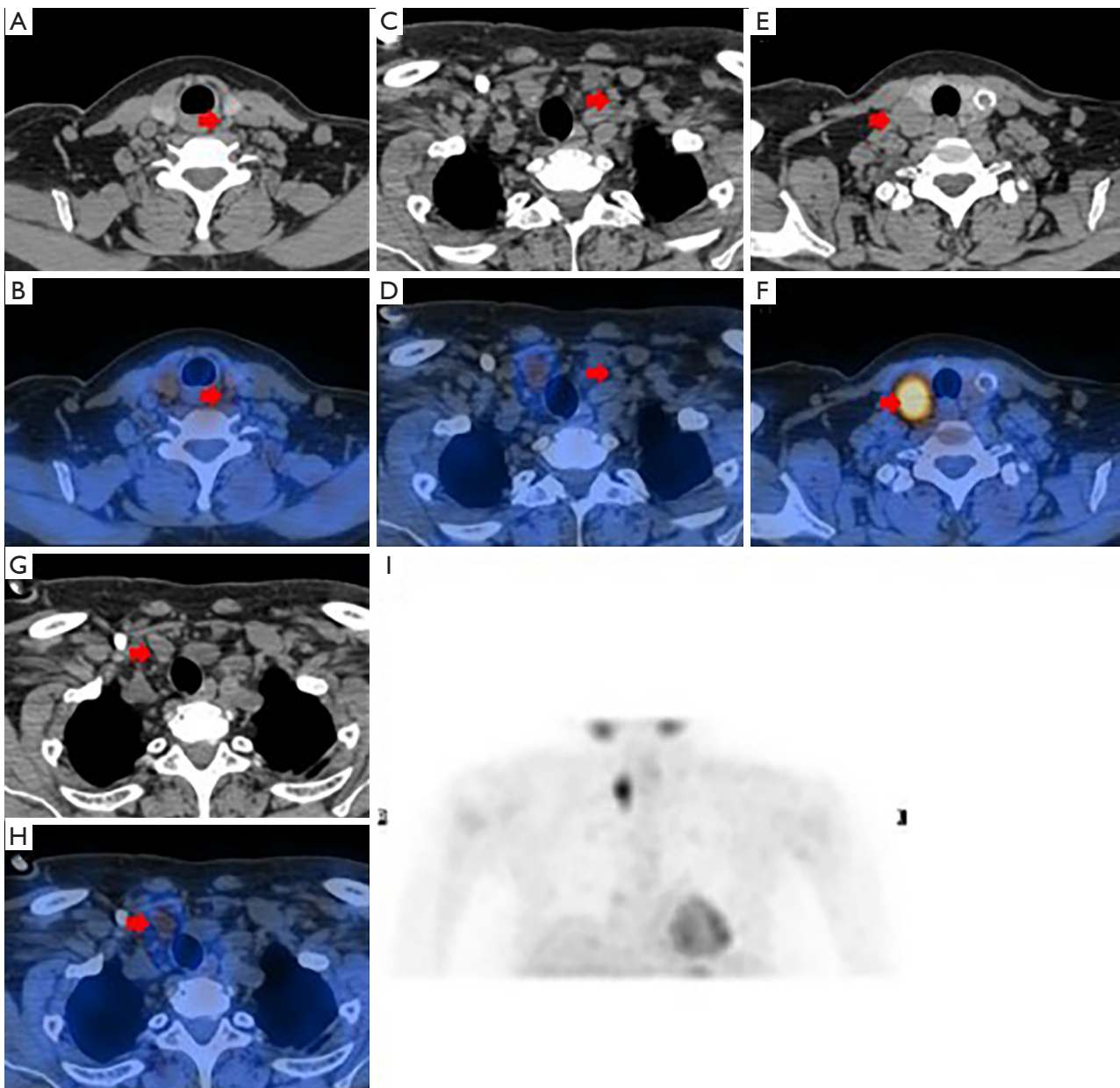


Figure 2 Axial CT (A,C,E,G) and SPECT/CT (B,D,F,H) showed four lesions in the back of the thyroid gland that were pathologically conformed to be parathyroid hyperplasia (A,B: superior left parathyroid gland, URRI =2.35; C,D: inferior left parathyroid gland, URRI =0.59; E,F: superior right parathyroid gland, URRI =8.03; G,H: inferior right parathyroid gland, URRI =3.62). The planar images (I) showed different ^{99m}Tc -MIBI uptake of the parathyroid glands in a patient. URRI, uptake ratio of region of interest.

images and the delayed phase (120 min). The radioactivity counts were obtained for the maximum cross lesion to represent ^{99m}Tc -MIBI uptake of lesions and the ipsilateral thymus, and the value of the uptake ratio of the region of interest (URRI) was calculated as the radioactivity count of the lesion divided by the ipsilateral thymus. ^{99m}Tc -MIBI

negative PG(s) patients had a URRI value of no more than 1; meanwhile, ^{99m}Tc -MIBI positive PG(s) patients had a URRI value of more than 1. The URRI total is the sum value of the URRI of all glands in a patient, and the URRI max is the maximum value of the URRI of all glands in a patient.

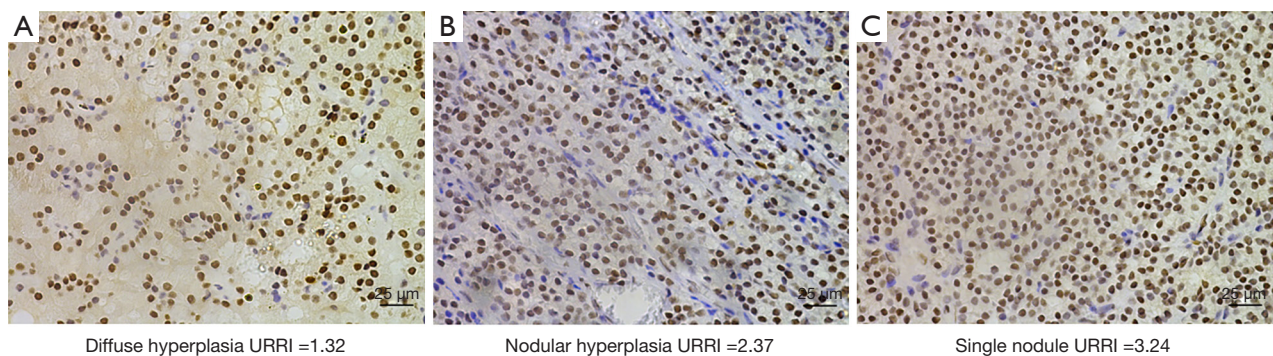


Figure 3 An example of PCNA staining (IHC) for different URRIs and degrees of pathological hyperplasia in different parathyroid glands of a patient. URR1, uptake ratio of region of interest; PCNA, proliferating cell nuclear antigen.

Immunohistochemistry (IHC)

The resected specimens were fixed in formaldehyde and embedded in paraffin. Sections (4 μm) were processed for hematoxylin and eosin and immunohistochemical staining. The sections were blocked with 3% hydrogen peroxide (H_2O_2) for 15 min to retrieve the enzyme for immunohistochemical staining. The sections were then treated with a sodium citrate buffer (pH 6.0; cat. no. C1010; Solarbio, Beijing, China) for 15 min at 95 $^\circ\text{C}$ and subsequently incubated with antibody proliferating cell nuclear antigen (PCNA) (1:5,000; cat no. 2586; Cell Signaling Technology, Danvers, MA, USA) at 4 $^\circ\text{C}$ overnight. After washing with Phosphate buffer saline (pH 7.2–7.4), the sections were incubated with anti-immunoglobulin G secondary antibody for 30 min at 37 $^\circ\text{C}$, and Diaminobezidin was added. Finally, the sections were washed under running water and stained with hematoxylin.

IHC analysis

Cells in sections expressing PCNA were counted using Leica DM4000 (Leica Inc., Germany) under 400 \times magnification, and five fields were selected randomly per section. We captured images of the fields using software program Leica Application Suite (version 8.0; Leica Inc., Germany). Each field was quantified using Image-Pro Plus software (version 6.0; MediaCybernetics, Inc., Rockville, MD, USA). The mean values are expressed as the number of positive cells per sample (Figure 3).

Statistical analysis

Statistical analysis of the anonymized database was

performed using SPSS version 22.0 software (IBM, Armonk, NY, USA). Descriptive statistics for continuous variables were presented as mean \pm standard deviation. Bivariate analysis was conducted with an independent sample *t*-test to compare the mean values. Categorical variables were expressed as numbers and percentages (%), and Fisher's chi-square test was used to assess the differences between groups. Binomial logistic regression analysis was used to assess the risk factors for hypocalcemia at 6 months postoperatively. The correlations between the URR1 value of PG and glandular weight, the URR1 value of PG and glandular volume, and the URR1 values of PG and PCNA were examined using linear regression analysis. The correlation between the URR1 value of PG and the hyperplastic pattern of PG was examined using one-way Analysis of Variance (ANOVA). A receiver operating characteristic (ROC) curve was used to validate the diagnostic tests, and to test the specificity and sensitivity, the area under the curve (AUC), standard error, and 95% confidence intervals (95% CI) were also calculated. Statistical significance was set at $P < 0.05$.

Results

The relationship between the $^{99\text{m}}\text{Tc}$ -MIBI information and clinical, biochemical results of 91 SHPT patients

The patient's demographics and clinical characteristics are shown in Table 1. Thirty-six (39.56%) patients exhibited $^{99\text{m}}\text{Tc}$ -MIBI negative parathyroid(s). The mean 6-month postoperative serum calcium of patients was 2.18 ± 0.26 mmol/L, categorized into two groups based on serum calcium levels (higher than or less than 2.11 mmol/L) at 6 months postoperatively with 36 patients

Table 1 Demographic and clinical characteristics of 91 patients who underwent total parathyroidectomy with autotransplantation

Characteristic	N or mean ± SD
Gender (%)	
Male	48 (52.75%)
Female	43 (47.25%)
Age (years)	49±10
Dialysis time (years)	7.69±3.19
Preoperative iPTH (pg/mL)	1,955.73±1,090.83
Postoperative iPTH (pg/mL)	16.31±36.74
iPTH at 6 months postoperatively (pg/mL)	58.89±104.97
Preoperative serum calcium (mmol/L)	2.44±0.23
Postoperative serum calcium (mmol/L)	2.12±0.22
Serum calcium at 6 months postoperatively (mmol/L)	2.18±0.26
Preoperative serum phosphorus (mmol/L)	2.03±0.44
Postoperative serum phosphorus (mmol/L)	1.21±0.46
Serum phosphorus at 6 months postoperatively (mmol/L)	1.30±0.45
URRI total	10.78±4.98
URRI max	4.51±2.50
Patients with ^{99m} Tc-MIBI negative parathyroid (s) (%)	36 (39.56%)
1	25 (27.47%)
2	7 (7.69%)
3	4 (4.40%)

iPTH, intact parathyroid hormone; URRI, uptake ratio of region of interest.

in the hypocalcemia group and 55 patients in the non-hypocalcemia group. ^{99m}Tc-MIBI negative PG(s) patients had lower preoperative serum phosphorus and higher serum calcium levels at 6 months postoperatively compared to ^{99m}Tc-MIBI positive PG(s) patients (all $P < 0.05$, *Table 2*).

The baseline characteristics, including sex, age, and time on dialysis, showed no difference between the two groups. No significant differences were detected between the two groups in terms of preoperative serum calcium ($P = 0.215$), postoperative serum calcium ($P = 0.452$), postoperative serum phosphorus ($P = 0.728$), postoperative iPTH ($P = 0.252$), serum phosphorus at 6 months postoperatively ($P = 0.126$), and iPTH at 6 months postoperatively ($P = 0.198$).

To clarify the risk factors for hypocalcemia at 6 months postoperatively in the entire cohort, patients were divided into two groups according to the occurrence of hypocalcemia at 6 months postoperatively (*Table 3*). In

the hypocalcemia group, the URRI total and URRI max were higher than those in the non-hypocalcemia group. Further multivariable logistic regression analysis was performed to analyze the association between the URRI value and hypocalcemia at 6 months postoperatively. Since the URRI max was significantly correlated with the URRI total, multivariable logistic regression analysis was performed separately. Both the URRI total (odds ratio = 0.857, $P = 0.003$) and URRI max (odds ratio = 0.779, $P = 0.028$) were independent risk factors for hypocalcemia at 6 months postoperatively (*Tables 4, 5*). Thus, a higher preoperative ^{99m}Tc-MIBI URRI value of the parathyroid indicated a higher incidence of hypocalcemia at 6 months postoperatively.

After subgroup analysis regarding whether to use the lowest URRI PG for autotransplantation, we found that the postoperative iPTH and iPTH levels at 6 months

Table 2 Demographic and clinical characteristics of patients with or without ^{99m}Tc -MIBI negative parathyroid gland(s)

Characteristic	Presence of ^{99m}Tc -MIBI negative parathyroid gland(s)		P value
	Yes (n=36)	No (n=55)	
Gender			0.393 ^x
Male	17	31	
Female	19	24	
Age* (years)	49±11	49±10	0.815 [†]
Dialysis time* (years)	7.37±3.35	7.90±3.11	0.442 [†]
Preoperative serum calcium* (mmol/L)	2.40±0.18	2.46±0.25	0.215 [†]
Preoperative serum phosphorus* (mmol/L)	1.89±0.44	2.12±0.43	0.015 [†]
Preoperative iPTH* (pg/mL)	1,690.08±1,078.42	2,129.60±1,073.10	0.060 [†]
Postoperative serum calcium* (mmol/L)	2.14±0.28	2.10±0.19	0.452 [†]
Postoperative serum phosphorus* (mmol/L)	1.19±0.41	1.22±0.49	0.728 [†]
Postoperative iPTH* (pg/mL)	10.83±18.50	19.90±44.67	0.252 [†]
Serum calcium at 6 months postoperatively* (mmol/L)	2.25±0.22	2.14±0.28	0.044 [†]
Serum phosphorus at 6 months postoperatively* (mmol/L)	1.39±0.47	1.24±0.43	0.126 [†]
iPTH 6 months postoperatively* (pg/mL)	41.32±72.40	70.39±120.94	0.198 [†]

[†], Two-tailed Student-Fisher *t*-test for unpaired data and equivalent variances; ^x, χ^2 test; *, mean ± SD; iPTH, intact parathyroid hormone.

Table 3 Demographic and clinical characteristics of patients who did or did not develop hypocalcemia at 6 months postoperatively

Characteristic	Hypocalcemia at 6 months postoperatively		P value
	Yes (n=36)	No (n=55)	
Gender			0.199 ^x
Male	16	32	
Female	20	23	
Age* (years)	52±9	47±11	0.059 [†]
Dialysis time* (years)	7.99±3.02	7.50±3.31	0.478 [†]
Preoperative serum calcium* (mmol/L)	2.46±0.23	2.43±0.23	0.464 [†]
Postoperative serum calcium* (mmol/L)	2.10±0.17	2.13±0.26	0.647 [†]
URRI total*	12.73±5.05	9.51±4.54	0.002 [†]
URRI max*	5.38±2.70	3.93±2.19	0.006 [†]

[†], two-tailed Student-Fisher *t*-test for unpaired data and equivalent variances; ^x, χ^2 test; *, mean ± SD; URRI, uptake ratio of region of interest.

postoperatively were all lower in the autotransplantation group with the lowest URRI PG (11.33±17.77 *vs.* 22.12±50.30, *P*=0.193; 41.59±68.50 *vs.* 79.07±133.87, *P*=0.106); however, the differences were not statistically significant (Table 6).

Relationship between the URRI value and the degree of pathological hyperplasia in 216 PGs

After analyzing all 216 PGs of 54 patients, the URRI values of the PGs were found to be significantly positively

Table 4 Multivariable logistic regression for risk factors of hypocalcemia at 6 months postoperatively

Variables	Coefficient	Standard error	P value	OR	95% confidence interval
Age (years)	-0.034	0.025	0.172	0.967	0.921–1.015
Postoperative serum calcium (mmol/L)	0.433	1.068	0.685	1.541	0.190–12.502
URRI total	-0.155	0.052	0.003	0.857	0.773–0.949

OR, odds ratio; URRI, uptake ratio of region of interest.

Table 5 Multivariable logistic regression for risk factors of hypocalcemia at 6 months postoperatively

Variables	Coefficient	Standard error	P value	OR	95% confidence interval
Age (years)	-0.028	0.024	0.258	0.973	0.927–1.020
Postoperative serum calcium (mmol/L)	0.262	1.047	0.803	1.299	0.167–10.105
URRI max	-0.249	0.114	0.028	0.779	0.624–0.974

OR, odds ratio; URRI, uptake ratio of region of interest.

Table 6 Demographic and clinical characteristics of patients who underwent autotransplantation with or without the lowest URRI parathyroid

Characteristic	Autotransplantation with lowest URRI parathyroid		P value
	Yes (n=49)	No (n=42)	
Postoperative serum calcium* (mmol/L)	2.11±0.20	2.12±0.26	0.740 ^x
Postoperative serum phosphorus* (mmol/L)	1.25±0.48	1.16±0.44	0.368 ^t
Postoperative iPTH* (pg/mL)	11.33±17.77	22.12±50.30	0.193 ^t
Serum calcium at 6 months postoperatively* (mmol/L)	2.18±0.24	2.18±0.29	0.993 ^t
Serum phosphorus at 6 months postoperatively* (mmol/L)	1.33±0.48	1.26±0.42	0.493 ^t
iPTH at 6 months postoperatively* (pg/mL)	41.59±68.50	79.07±133.87	0.106 ^t

^t, two-tailed Student-Fisher *t*-test for unpaired data and equivalent variances; ^x, χ^2 test; *, mean ± SD; URRI, uptake ratio of region of interest.

correlated with glandular weight ($R^2=0.343$, $P<0.001$), glandular volume ($R^2=0.240$, $P<0.001$), and degree of pathological hyperplasia ($P<0.001$) (Figure 4). However, the URRI value of the PGs exhibited a notably weak correlation with PCNA ($R^2=0.035$, $P=0.006$). These results indicate that ^{99m}Tc-MIBI imaging is closely related to the pathological hyperplasia of the PG.

The location of the 216 PGs was precisely divided into superior and inferior groups first according to anatomy, followed by the midline of the thyroid. Compared to the inferior PGs, the superior glands were more similar to the normal PG in terms of the following: degree of pathological hyperplasia ($P=0.029$), lighter weight ($P=0.002$), smaller volume ($P<0.001$), and less PCNA staining ($P=0.004$) (Table 7).

At the end of the study, the AUC of the ROC curves

showed a URRI evaluative value of 0.771 (Figure 5A, Table 8) for diffuse and nodular types in the 216 PGs ($P<0.001$). During the evaluation of the nodular subtype (distinguishing between nodular hyperplasia and single nodule), the URRI evaluative value even reached 0.819 (Figure 5B, Table 9), which was higher than the volume or weight in 167 nodular-type PGs ($P<0.001$).

Discussion

Surgical treatments play a key role in the management of SHPT (5,17–19), and preoperative positioning of hyperplastic PGs is crucial for surgical treatment. The importance of ^{99m}Tc-MIBI imaging in SHPT has been well documented in numerous studies and guidelines (13,20,21). It is worth noting that ^{99m}Tc-MIBI-guided

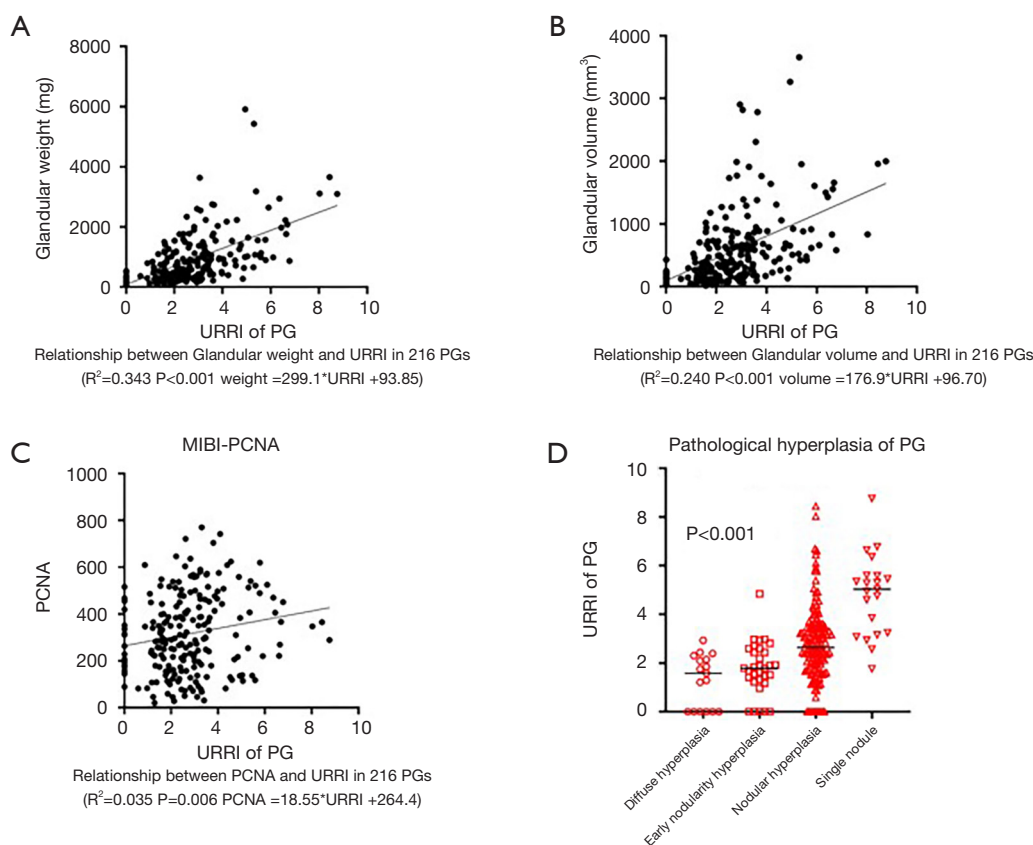


Figure 4 The relationship between the value of parathyroid URRI and glandular weight (A), glandular volume (B), PCNA (C), and pathological hyperplasia of PG (D). URRI, uptake ratio of region of interest; PCNA, proliferating cell nuclear antigen.

Table 7 Specimen characteristics of parathyroid glands

Characteristic	The location of the parathyroid glands		P value
	Superior (n=108)	Inferior (n=108)	
Pathological hyperplasia			0.029 ^x
Diffuse hyperplasia	12 (11.11%)	5 (4.63%)	
Early nodularity hyperplasia	20 (18.52%)	12 (11.11%)	
Nodular hyperplasia	70 (64.81%)	76 (70.37%)	
Single nodule hyperplasia	6 (5.56%)	15 (13.89%)	
Weight* (mg)	724.10±712.59	1,086.06±955.92	0.002 [†]
Volume* (mm ³)	418.13±457.30	734.55±696.02	<0.001 [†]
URRI*	2.57±1.69	2.86±1.67	0.209 [†]
^{99m} Tc-MIBI -/+ (URRI >1)	14/94	11/97	0.523 ^x
PCNA*	281.81±140.58	347.63±184.31	0.004 [†]

[†], two-tailed Student-Fisher *t*-test for unpaired data and equivalent variances; ^x, χ^2 test; *, mean ± SD; URRI, uptake ratio of region of interest; PCNA, proliferating cell nuclear antigen.

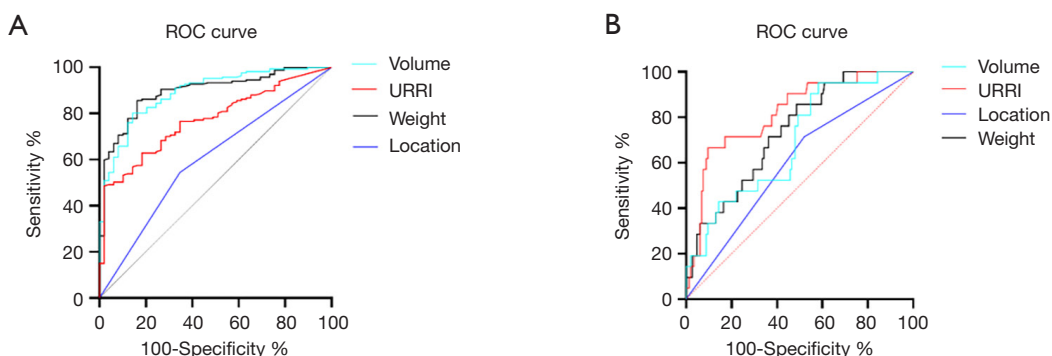


Figure 5 ROC curves demonstrating (A) the accuracy of volume, URRI, weight, and location as predictors of diffuse and nodular types in 216 parathyroid glands, and (B) the accuracy of volume, URRI, weight, and location as predictors of nodular hyperplasia and single nodule in 167 parathyroid glands with nodular-type. URRI, uptake ratio of region of interest.

Table 8 Evaluative performance for a nodular type in 216 parathyroid glands

Factors	AUC	Standard error	95% CI	P value
Location	0.599	0.046	0.510–0.688	0.035
URRI	0.771	0.034	0.706–0.837	<0.001
Volume	0.890	0.025	0.842–0.939	<0.001
Weight	0.895	0.024	0.848–0.942	<0.001

URRI, uptake ratio of region of interest; AUC, area under the curve.

Table 9 Evaluative performance for a single nodule in 167 nodular-type parathyroid glands

Factors	AUC	Standard error	95% CI	P value
Location	0.597	0.064	0.472–0.722	0.152
URRI	0.819	0.048	0.725–0.913	<0.001
Volume	0.692	0.058	0.578–0.805	0.005
Weight	0.735	0.052	0.633–0.837	<0.001

URRI, uptake ratio of region of interest; AUC, area under the curve.

parathyroidectomy can better assist surgeons in locating parathyroids more easily, removing all hyperplastic parathyroids, as well as improving PTH, blood calcium, and phosphorus levels (22). We have been investigating the relationship between ^{99m}Tc-MIBI imaging semi-quantitative analysis and hyperplastic PGs, applying this to clinical practice to improve the diagnosis and treatment of SHPT patients.

Initially, we found that patients with ^{99m}Tc-MIBI-negative PGs (particularly those with more than one negative PG) often show lower PTH levels and lower intraoperative parathyroid gland hyperplasia (PGH). Most of the ^{99m}Tc-

MIBI-negative PGs were close to normal in pathological hyperplasia. These results confirm our hypothesis: patients with ^{99m}Tc-MIBI-negative PGs demonstrate lower serum phosphorus and iPTH levels preoperatively, while patients with all positive PGs imaging exhibit more severe SHPT. In addition, the difficulty of surgery is greatly reduced for surgeons when a patient's preoperative ^{99m}Tc-MIBI imaging clearly shows the PG locations. Therefore, combining the specific characteristics of each patient (including preoperative iPTH, state of dialysis and kidney transplantation, drug resistance, etc.) with their ^{99m}Tc-MIBI imaging can help doctors determine the need for surgery

and the optimal operation time. Moreover, it can also avoid unnecessary total or SPTX due to no PG being found, and increase the success rate of surgery.

For SHPT patients, hypocalcemia is one of the most common complications after PTX (23). Although we have given priority to the postoperative monitoring and management of serum calcium levels, the incidence of hypocalcemia after PTX remains high (24,25). Hypocalcemia is the reduction of calcium from circulation (26). Severe hypocalcemia can cause bone loss, tremors in the hands and feet, cardiac arrhythmia, and sudden death, and therefore, early prevention and prompt treatment are required.

Patients who underwent TPTX+AT were followed up, and we found that ^{99m}Tc -MIBI-positive PG(s) patients showed lower serum calcium levels at 6 months postoperatively compared to ^{99m}Tc -MIBI-negative PG(s) patients. Therefore, we conducted further analysis to quantify the ^{99m}Tc -MIBI imaging of the PGs, and subgroup analysis was performed according to the occurrence of hypocalcemia (at 6 months postoperatively). Further verification showed that the patients' URRI max and URRI total (collectively referred to as URRI) were negatively correlated with serum calcium levels 6 months postoperatively. Patients with higher URRI values were more likely to have hypocalcemia at 6 months postoperatively than patients with lower URRI values. This indicates that patients with obvious ^{99m}Tc -MIBI scintigraphic visualization have a worse prognosis, and timely medical operations should be performed for these patients.

In general, both SPTX and TPTX+AT require selecting the partial PG tissue with the lowest degree of hyperplasia among all PGs for preservation *in situ* or autotransplantation (27,28). According to the classification of pathological hyperplasia of the PG in SHPT, hyperplastic PGs are divided into two types: diffuse type (which has a lower degree of hyperplasia) and nodular type (which have a higher degree of hyperplasia). The diffuse type includes diffuse hyperplasia and early nodular hyperplasia, while the nodular type includes nodular hyperplasia and a single nodule (29). The hyperplastic parathyroid tissue is heterogeneous. Removal of PGH by intraoperative frozen section diagnosis cannot represent transplanted PGH. When performing SPTX, the selected PG needs to be preserved *in situ*, which increases the difficulty in evaluating the degree of hyperplasia. All of the above factors could interfere with our judgment of the hyperplastic

degree of the partial gland to be left. Typically, in clinical practice, the partial PG to be left is chosen based on an intraoperative frozen diagnosis of another partial PG that has been resected, combined with visual judgment or even intraoperative magnification judgment (27,30). In this study, we found that the analysis of ^{99m}Tc -MIBI imaging helps in evaluating the degree of PGH before surgery and selecting the partial parathyroid tissue (with the lowest degree of hyperplasia) for preservation *in situ* or autotransplantation in surgery.

During the embryonic development of PGs, inferior PGs originate from the third pharyngeal pouches, while the superior PGs originate from the fourth pharyngeal pouch. Therefore, the anatomical origins of the superior and inferior PGs differ (31,32), which drew our attention to the difference between the superior and inferior PGs. We found that the superior PGs tended to have a lighter weight, smaller volume, lower PCNA expression, and lower degree of hyperplasia. Our preoperative ^{99m}Tc -MIBI imaging showed that the degree of visualization of the superior PGs was lower, consistent with previous research (33). This may be due to the effect of hemodynamics, gravity, and a relatively narrow growth area, leading to slower pathological growth in the superior PGs than in the inferior PGs (32). From this perspective, we could select the superior PGs for preservation if a dilemma in selecting PG arises intraoperatively.

Analysis of the 216 PGs of 54 patients verified our hypothesis that ^{99m}Tc -MIBI imaging is associated with the pathological characteristics of the PGs in SHPT, including weight, volume, PCNA expression, and degree of pathological hyperplasia. Therefore, evaluating the degree of PGH by preoperative ^{99m}Tc -MIBI imaging could help to select the PG and leave it *in situ* following specific conditions during the operation. Our study implied that when the degree of pathological hyperplasia of the PGs was divided into three types: nodular hyperplasia, single nodule, and diffuse type (including diffuse hyperplasia and early nodular hyperplasia), the URRI had a better evaluative value for the degree of PGH (AUC =0.771). Meanwhile, the 167 PGs of the nodular type were divided into nodular hyperplasia and single nodule, the URRI's evaluative value of PGH was better than that of the naked eye on the appearance of the PG (including weight, volume, etc.). It is worth noting that this information could be obtained through ^{99m}Tc -MIBI imaging preoperatively, which could help achieve optimal preoperative preparation.

However, this study has several limitations that should be

noted. In terms of design, due to the limitations of diagnosis and treatment standards, we had to select the partial parathyroid tissue (with the lowest degree of hyperplasia) for autotransplantation according to the surgeon's experience. The design of a prospective control study to compare different ^{99m}Tc-MIBI imaging accumulations is against the ethics and guidelines. Also, the sample size in this study was relatively small, and it was a single-center study. Considering these limitations, we hope to conduct a prospective randomized controlled study with large sample size and long follow-up period in the future to confirm our research conclusions.

Conclusions

In general, in addition to the parathyroid location, the ^{99m}Tc-MIBI scintigraphy results were related to the serum calcium level at 6 months after TPTX+AT, suggesting the occurrence of hypocalcemia (6 months after TPTX+AT). More importantly, this technique effectively evaluates the pathological hyperplasia of the PGs preoperatively, and therefore, could assist surgeons in selecting the PG with the lowest degree of hyperplasia intraoperatively.

Acknowledgments

Funding: This study was supported by grants from the National Natural Science Foundation of China (No. 81772853, 81972495, and 81902719), the National Natural Science Foundation of Zhejiang (No. LY18H160012 and LQ18H120002), and the Key Project of Scientific and Technological Innovation of Zhejiang Province (No. 2015C03031).

Footnote

Conflicts of Interest: All the authors have completed the ICMJE uniform disclosure form (available at <http://dx.doi.org/10.21037/qims-21-66>). The authors have no conflicts of interest to declare.

Ethical Statement: The authors are accountable for all aspects of the work in ensuring that questions related to the accuracy or integrity of any part of the work are appropriately investigated and resolved. This study was conducted in accordance with the Declaration of Helsinki (as revised in 2013), and was approved by institutional of Clinical Research Ethics Committee of the First Affiliated

Hospital, Zhejiang University School of Medicine (No. IIT20200715). The requirement for individual consent for this retrospective analysis was waived.

Open Access Statement: This is an Open Access article distributed in accordance with the Creative Commons Attribution-NonCommercial-NoDerivs 4.0 International License (CC BY-NC-ND 4.0), which permits the non-commercial replication and distribution of the article with the strict proviso that no changes or edits are made and the original work is properly cited (including links to both the formal publication through the relevant DOI and the license). See: <https://creativecommons.org/licenses/by-nc-nd/4.0/>.

References

1. Portillo MR, Rodríguez-Ortiz ME. Secondary Hyperparathyroidism: Pathogenesis, Diagnosis, Preventive and Therapeutic Strategies. *Rev Endocr Metab Disord* 2017;18:79-95.
2. Hsu CY, Chen LR, Chen KH. Osteoporosis in Patients with Chronic Kidney Diseases: A Systemic Review. *Int J Mol Sci* 2020;21:6846.
3. Zawierucha J, Malyszko J, Malyszko JS, Prystacki T, Marcinkowski WP, Dryl-Rydzynska T. Three Therapeutic Strategies: Cinacalcet, Paricalcitol or Both in Secondary Hyperparathyroidism Treatment in Hemodialysed Patients During 1-Year Observational Study-A Comparison. *Front Endocrinol (Lausanne)* 2019;10:40.
4. Block GA, Bushinsky DA, Cunningham J, Druke TB, Ketteler M, Kewalramani R, Martin KJ, Mix TC, Moe SM, Patel UD, Silver J, Spiegel DM, Sterling L, Walsh L, Chertow GM. Effect of Etelcalcetide vs Placebo on Serum Parathyroid Hormone in Patients Receiving Hemodialysis With Secondary Hyperparathyroidism: Two Randomized Clinical Trials. *JAMA* 2017;317:146-55.
5. Lau WL, Obi Y, Kalantar-Zadeh K. Parathyroidectomy in the Management of Secondary Hyperparathyroidism. *Clin J Am Soc Nephrol* 2018;13:952-61.
6. Isakova T, Nickolas TL, Denburg M, Yarlagadda S, Weiner DE, Gutiérrez OM, Bansal V, Rosas SE, Nigwekar S, Yee J, Kramer H. KDOQI US Commentary on the 2017 KDIGO Clinical Practice Guideline Update for the Diagnosis, Evaluation, Prevention, and Treatment of Chronic Kidney Disease-Mineral and Bone Disorder (CKD-MBD). *Am J Kidney Dis* 2017;70:737-51.
7. Schlosser K, Bartsch DK, Diener MK, Seiler CM, Bruckner T, Nies C, Meyer M, Neudecker J, Goretzki

- PE, Glockzin G, Konopke R, Rothmund M. Total Parathyroidectomy With Routine Thymectomy and Autotransplantation Versus Total Parathyroidectomy Alone for Secondary Hyperparathyroidism: Results of a Nonconfirmatory Multicenter Prospective Randomized Controlled Pilot Trial. *Ann Surg* 2016;264:745-53.
8. Albuquerque RFC, Carbonara CEM, Martin RCT, Dos Reis LM, do Nascimento CP Júnior, Arap SS, Moysés RMA, Jorgetti V, Montenegro FLM, de Oliveira RB. Parathyroidectomy in patients with chronic kidney disease: Impacts of different techniques on the biochemical and clinical evolution of secondary hyperparathyroidism. *Surgery* 2018;163:381-7.
 9. Jäger MD, Serttas M, Beneke J, Müller JA, Schrem H, Kaltenborn A, Ramackers W, Ringe BP, Gwiasda J, Tränkenschuh W, Klempnauer J, Scheumann GFW. Risk-factors for nodular hyperplasia of parathyroid glands in sHPT patients. *PLoS One* 2017;12:e0186093.
 10. Melck AL, Carty SE, Seethala RR, Armstrong MJ, Stang MT, Ogilvie JB, Yip L. Recurrent hyperparathyroidism and forearm parathyromatosis after total parathyroidectomy. *Surgery* 2010;148:867-73; discussion 873-5.
 11. Yumita S. Intervention for recurrent secondary hyperparathyroidism from a residual parathyroid gland. *Nephrol Dial Transplant* 2003;18 Suppl 3:iii62-4.
 12. Monzen Y, Tamura A, Okazaki H, Kurose T, Kobayashi M, Kuraoka M. SPECT/CT Fusion in the Diagnosis of Hyperparathyroidism. *Asia Ocean J Nucl Med Biol* 2015;3:61-5.
 13. Jiang SQ, Yang T, Zou Q, Xu L, Ye T, Kang YQ, Li WR, Jiao J, Zhang Y. The role of 99mTc-MIBI SPECT/CT in patients with secondary hyperparathyroidism: comparison with 99mTc-MIBI planar scintigraphy and ultrasonography. *BMC Med Imaging* 2020;20:115.
 14. Kara M, Tellioglu G, Bugan U, Krand O, Berber I, Seymen P, Eren PA, Ozel L, Titiz I. Evaluation of intraoperative parathormone measurement for predicting successful surgery in patients undergoing subtotal/total parathyroidectomy due to secondary hyperparathyroidism. *Laryngoscope* 2010;120:1538-44.
 15. Al Rukhaimi M, Al Sahow A, Boobes Y, Goldsmith D, Khabouth J, El Baz T, Mahmoud H, Ganji MR, Shaheen FA; Kidney Disease: Improving Global Outcomes. Adaptation and implementation of the "Kidney Disease: Improving Global Outcomes (KDIGO)" guidelines for evaluation and management of mineral and bone disorders in chronic kidney disease for practice in the Middle East countries. *Saudi J Kidney Dis Transpl* 2014;25:133-48.
 16. Casella C, Galani A, Totaro L, Ministrini S, Lai S, Dimko M, Portolani N. Total Parathyroidectomy with Subcutaneous Parathyroid Forearm Autotransplantation in the Treatment of Secondary Hyperparathyroidism: A Single-Center Experience. *Int J Endocrinol* 2018;2018:6065720.
 17. Delos Santos R, Rossi A, Coyne D, Maw TT. Management of Post-transplant Hyperparathyroidism and Bone Disease. *Drugs* 2019;79:501-13.
 18. Almquist M, Isaksson E, Clyne N. The treatment of renal hyperparathyroidism. *Endocr Relat Cancer* 2020;27:R21-34.
 19. Eidman KE, Wetmore JB. The role of parathyroidectomy in the management of secondary hyperparathyroidism. *Curr Opin Nephrol Hypertens* 2017;26:516-22.
 20. Kushchayeva YS, Tella SH, Kushchayev SV, Van Nostrand D, Kulkarni K. Comparison of hyperparathyroidism types and utility of dual radiopharmaceutical acquisition with Tc99m sestamibi and 123I for localization of rapid washout parathyroid adenomas. *Osteoporos Int* 2019;30:1051-7.
 21. Fukagawa M, Yokoyama K, Koiwa F, Taniguchi M, Shoji T, Kazama JJ, et al. Clinical practice guideline for the management of chronic kidney disease-mineral and bone disorder. *Ther Apher Dial* 2013;17:247-88.
 22. Chen J, Feng J, Zhou Q, Zheng W, Meng X, Wang Y, Wang J. Intraoperative 99mTc-MIBI-Guided Parathyroidectomy Improves Curative Effect of Parathyroidectomy, Bone Metabolism, and Bone Mineral Density. *Am Surg* 2021;87:463-72.
 23. Unsal IO, Calapkulu M, Sencar ME, Hepsen S, Sakiz D, Ozbek M, Cakal E. Preoperative Vitamin D Levels as a Predictor of Transient Hypocalcemia and Hypoparathyroidism After Parathyroidectomy. *Sci Rep* 2020;10:9895.
 24. Tsai WC, Peng YS, Chiu YL, Wu HY, Pai MF, Hsu SP, Yang JY, Tung KT, Chen HY. Risk factors for severe hypocalcemia after parathyroidectomy in prevalent dialysis patients with secondary hyperparathyroidism. *Int Urol Nephrol* 2015;47:1203-7.
 25. Wei Y, Yu MA, Qian LX, Zhao ZL, Cao XJ, Peng LL, Li Y. Hypocalcemia after ultrasound-guided microwave ablation and total parathyroidectomy for secondary hyperparathyroidism: a retrospective study. *Int J Hyperthermia* 2020;37:819-25.
 26. Mazzaferro S, Chicca S, Pasquali M, Zaraca F, Ballanti P, Taggi F, Coen G, Cinotti GA, Carboni M. Changes in bone turnover after parathyroidectomy in dialysis patients: role of calcitriol administration. *Nephrol Dial Transplant*

- 2000;15:877-82.
27. Xu D, Yin Y, Hou L, Dai W. Surgical management of secondary hyperparathyroidism: how to effectively reduce recurrence at the time of primary surgery. *J Endocrinol Invest* 2016;39:509-14.
 28. Ohta K, Manabe T, Katagiri M, Harada T. Expression of proliferating cell nuclear antigens in parathyroid glands of renal hyperparathyroidism. *World J Surg* 1994;18:625-8; discussion 628-9.
 29. Tominaga Y, Tanaka Y, Sato K, Nagasaka T, Takagi H. Histopathology, pathophysiology, and indications for surgical treatment of renal hyperparathyroidism. *Semin Surg Oncol* 1997;13:78-86.
 30. Neyer U, Hoerandner H, Haid A, Zimmermann G, Niederle B. Total parathyroidectomy with autotransplantation in renal hyperparathyroidism: low recurrence after intra-operative tissue selection. *Nephrol Dial Transplant* 2002;17:625-9.
 31. Boyd JD. Development of the thyroid and parathyroid glands and the thymus. *Ann R Coll Surg Engl* 1950;7:455-71.
 32. Uludağ M, Aygün N, İşgör A. Main Surgical Principles and Methods in Surgical Treatment of Primary Hyperparathyroidism. *Sisli Etfal Hastan Tip Bul* 2019;53:337-52.
 33. Lomonte C, Buonvino N, Selvaggiolo M, Dassira M, Grasso G, Vernaglione L, Basile C. Sestamibi scintigraphy, topography, and histopathology of parathyroid glands in secondary hyperparathyroidism. *Am J Kidney Dis* 2006;48:638-44.

Cite this article as: Ma J, Yang J, Chen C, Lu Y, Mao Z, Wang H, Yang Y, Li Z, Wang W, Teng L. Use of ^{99m}Tc-sestamibi SPECT/CT imaging in predicting the degree of pathological hyperplasia of the parathyroid gland: semi-quantitative analysis. *Quant Imaging Med Surg* 2021;11(10):4375-4388. doi: 10.21037/qims-21-66